Volume 9
Number 15
7 August 2021
Pages 5059-5386

# Biomaterials Science

rsc.li/biomaterials-science

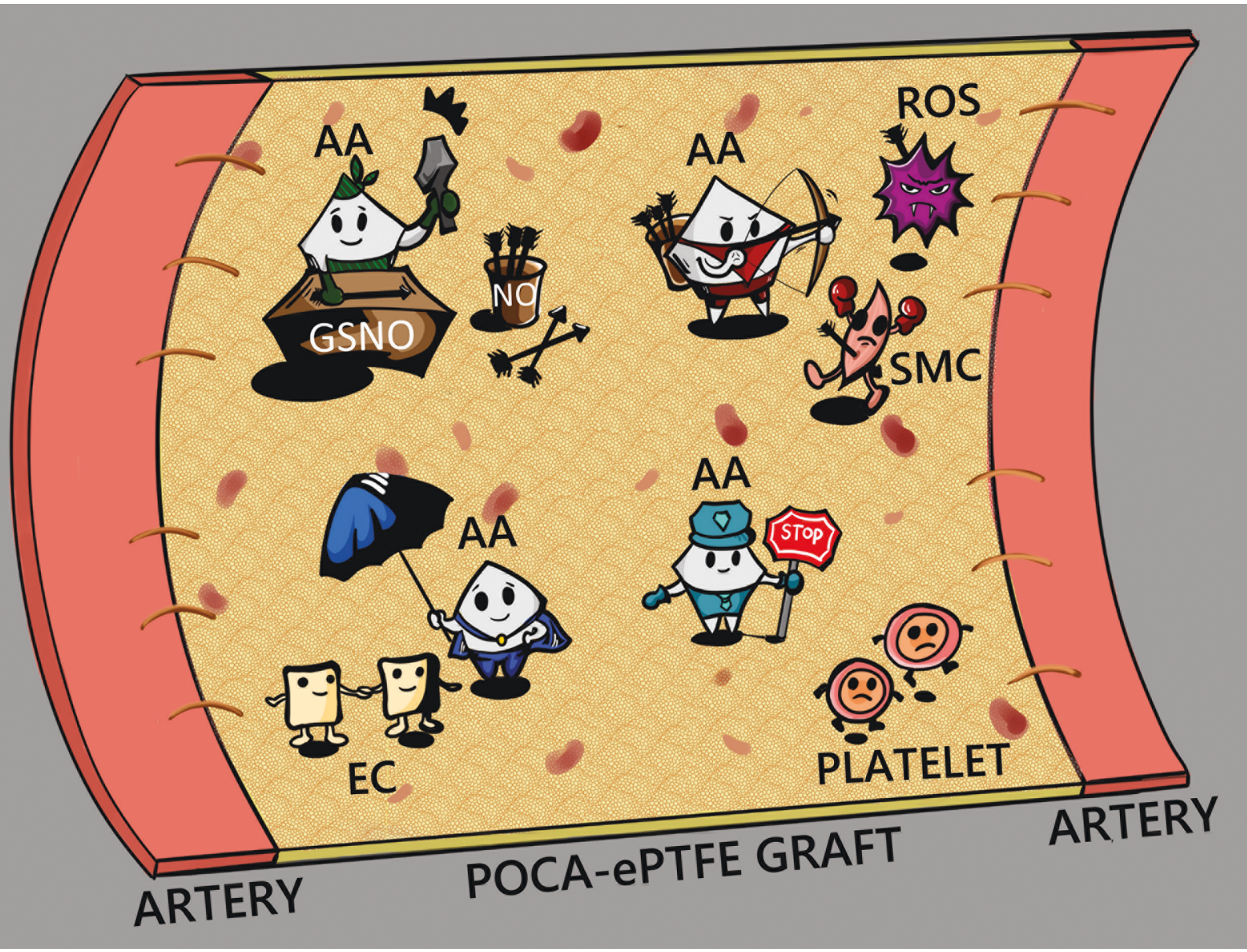


ISSN 2047-4849

ROYAL SOCIETY OF CHEMISTRY

**PAPER**
Melina R. Kibbe *et al.*
Coating small-diameter ePTFE vascular grafts with tunable poly(diol-*co*-citrate-*co*-ascorbate) elastomers to reduce neointimal hyperplasia

European Society for Biomaterials

Biomaterials Science

ROYAL SOCIETY OF CHEMISTRY

PAPER

View Article Online
View Journal | View Issue



Cite this: *Biomater. Sci.*, 2021, **9**, 5160

# Coating small-diameter ePTFE vascular grafts with tunable poly(diol-*co*-citrate-*co*-ascorbate) elastomers to reduce neointimal hyperplasia†

Lu Yu, [a] Emily R. Newton,[a] David C. Gillis,[a] Kui Sun,[a] Brian C. Cooley,[b] Andrew N. Keith,[c] Sergei S. Sheiko,[c] Nick D. Tsihlis [a] and Melina R. Kibbe *[a,d,e]

Lack of long-term patency has hindered the clinical use of small-diameter prosthetic vascular grafts with the majority of these failures due to the development of neointimal hyperplasia. Previous studies by our laboratory revealed that small-diameter expanded polytetrafluoroethylene (ePTFE) grafts coated with antioxidant elastomers are a promising localized therapy to inhibit neointimal hyperplasia. This work is focused on the development of poly(diol-*co*-citrate-*co*-ascorbate) (POCA) elastomers with tunable properties for coating ePTFE vascular grafts. A bioactive POCA elastomer (@20 : 20 : 8, [citrate] : [diol] : [ascorbate]) coating was applied on a 1.5 mm diameter ePTFE vascular graft as the most promising therapeutic candidate for reducing neointimal hyperplasia. Surface ascorbate density on the POCA elastomer was increased to 67.5 ± 7.3 ng mg$^{-1}$ cm$^{-2}$. The mechanical, antioxidant, biodegradable, and biocompatible properties of POCA demonstrated desirable performance for *in vivo* use, inhibiting human aortic smooth muscle cell proliferation, while supporting human aortic endothelial cells. POCA elastomer coating number was adjusted by a modified spin-coating method to prepare small-diameter ePTFE vascular grafts similar to natural vessels. A significant reduction in neointimal hyperplasia was observed after implanting POCA-coated ePTFE vascular grafts in a guinea pig aortic interposition bypass graft model. POCA elastomer thus offers a new avenue that shows promise for use in vascular engineering to improve long-term patency rates by coating small-diameter ePTFE vascular grafts.

Received 19th January 2021,
Accepted 27th March 2021

DOI: 10.1039/d1bm00101a

rsc.li/biomaterials-science



## 1. Introduction

Cardiac and peripheral artery bypass grafting remain commonly performed vascular surgeries worldwide and are forecast to continue to increase in the near future.[1–3] The ability of vascular grafts to prevent thrombosis, inhibit neointimal hyperplasia, and promote re-endothelialization significantly determines the long-term clinical outcomes of vascular grafts. Autologous vessels (*i.e.*, internal thoracic artery, greater saphenous vein, *etc.*) remain the gold standard conduits for bypass grafting, especially for small vessels (internal diameter < 6 mm). However, patients often have underlying conditions or have undergone prior harvesting procedures that leave insufficient autologous conduits for surgical treatment. Synthetic materials, such as expanded polytetrafluoroethylene (ePTFE), are often utilized as vascular graft substitutes in these situations, though there are more favorable replacements for large-diameter vessels. For small-diameter ePTFE vascular grafts, acute thrombotic events, neointimal thickening that narrows or occludes the graft, and a lower tendency to regenerate a functional endothelial layer cause them to fail when used off-the-shelf.[4–6] Poly(glycerol sebacate) (PGS), polycaprolactone (PCL), and hybrid biomaterials combined with decellularized matrices as regenerative design strategies have been used to improve the performance of small diameter vascular grafts.[7–10] To improve long-term durability, small-diameter ePTFE graft lumen modification constitutes a major area of current research with different strategies.[11–13] Biomolecules such as heparin,[14] growth factor,[15] homing factor,[16] extracellular matrix and elastin,[17,18] and autologous endothelial cells and

[a]*Department of Surgery, University of North Carolina at Chapel Hill, 4001 Burnett-Womack Building, CB #7050, Chapel Hill, NC 27599-7050, USA. E-mail: melina_kibbe@med.unc.edu; Tel: +1 919-445-0369*
[b]*Department of Pathology and Laboratory Medicine, University of North Carolina at Chapel Hill, Brinkhous-Bullitt Building, CB #7525, Chapel Hill, NC 27599-7525, USA*
[c]*Department of Chemistry, University of North Carolina at Chapel Hill, CB #3290, Chapel Hill, NC 27599-3290, USA*
[d]*Department of Biomedical Engineering, University of North Carolina at Chapel Hill, 10010 Mary Ellen Jones Building, CB #7575, Chapel Hill, NC 27599-7575, USA*
[e]*Surgical Services, Department of Veterans Affairs Medical Center, Durham, NC 27705, USA*

†Electronic supplementary information (ESI) available. See DOI: 10.1039/d1bm00101a

their progenitors,[19–21] have been combined with physicochemical modification methods and tissue engineering techniques to improve graft endothelialization to overcome graft failure induced by thrombosis or neointimal hyperplasia. However, the complex chemistry procedures with low surface modification efficiency and the lack of homogenous surface modifications have limited clinical adoption of small-diameter modified ePTFE grafts.

As a special class of thermoset polymeric materials, poly(diol-*co*-citrate) (PDC) is favorable for its intrinsic elastomeric, biodegradable, and biocompatible properties with poly(1,8-octanediol-*co*-citrate) (POC) developed as a powerful tool for vascular engineering.[22–24] Relative to other biomaterials, POC covers a suitable range of mechanical properties, degradation rates, hemocompatibility, and allows for incorporating a variety of therapeutic molecules in its polymer structure including antioxidant, antimicrobial, adhesive, and fluorescent molecules.[25,26] Antioxidant components have been incorporated in POC networks as a strategy for small-diameter ePTFE graft luminal surface modification.[27–30] For example, all-*trans* retinoic acid (atRA) was immobilized on small-diameter ePTFE grafts coated with POC by physisorption.[27] Poly(1,8-octanediol-*co*-citrate-*co*-ascorbate) (POCA) was synthesized by mixing citric acid, 1,8-octanediol, and ascorbic acid at a maximum mole feeding ratio (@5 : 5 : 1, [citrate] : [diol] : [ascorbate]) to prepare a superior antioxidant elastomer.[28] Both atRA-POC and POCA have been used on small-diameter ePTFE grafts, and *in vivo* studies demonstrate a visibly reduced neointimal hyperplasia compared to untreated equivalents.[27,28] Cumulatively, the previous studies strongly suggest that modification of small-diameter ePTFE grafts *via* coating with therapeutic elastomers has a significant potential to inhibit neointimal hyperplasia and reduce the risk of graft failure.

Ascorbic acid has been considered a key cellular antioxidant to scavenge radicals, and localized delivery of ascorbic acid has been expected to act as a therapeutic method to overcome the poor patency rate of small-diameter ePTFE grafts.[31,32] Several *in vitro* and *in vivo* studies have noted ascorbic acid has the potential to prevent endothelial cell (EC) apoptosis;[33] inhibit reactive oxygen species (ROS)-induced vascular smooth muscle cell (VSMC) activation, migration, and over-proliferation;[34] and was identified as a co-factor[35] for enhancing endogenous nitric oxide synthase (eNOS) activity. In clinical trials, administration of ascorbic acid has been shown to be beneficial to endothelial function of patients with endothelial dysfunction caused by hypertension, smoking, and diabetes.[36,37] However, due to the intrinsic properties of ascorbic acid, such as water-solubility and environmental sensitivity, localized ascorbate delivery by surface modification techniques like plasma treatment poses different challenges compared to physically or covalently immobilized ascorbate on the lumen of ePTFE grafts.

We previously reported a synthetic route for an ascorbate-bearing polymer (POCA) by inducing protection/deprotection steps for maximum loading of active ascorbate. The ascorbate was well shielded during POCA prepolymer preparation, and the moldable POCA elastomer exhibited enhanced ascorbate performance.[30] In the present study, we employed the same strategy and, by precisely controlling the mole feeding ratio of citrate, diol, and benzyl-protected ascorbate, we tuned the properties of POCA prepolymers and elastomers over a series of ascorbate compositions. We hypothesized that ascorbate plays a multifunctional role in the process to maintain small-diameter ePTFE vascular graft long-term patency, acting as an antioxidant, an antiproliferative, and an anti-adhesive against smooth muscle cell (SMC), and decomposing *S*-nitrosoglutathione (GSNO) to release nitric oxide. Following extensive studies, we identified the most therapeutic POCA elastomer candidate (@20 : 20 : 8, [citrate] : [diol] : [ascorbate]) and coated it onto a small-diameter ePTFE vascular graft. We tested the ability of the POCA-ePTFE graft to inhibit neointimal hyperplasia in a guinea pig aortic interposition bypass model.

## 2. Materials and methods

Unless otherwise indicated, all reagents were purchased from Sigma-Aldrich (St Louis, MO, USA) and all solvents were ACS grade or higher. 2,3-benzyl-ascorbate was synthesized as previously reported.[30]

### 2.1 Prepolymer preparation and characterization

POCA prepolymers were prepared as previously reported with modification.[30] In brief, POCA prepolymers were synthesized by mixing citric acid (CA), 1,8-octanediol (OD), and 2,3-benzyl-ascorbate (AA-Bn) in a range of mole feeding ratios (typical example for [CA] : [OD] : [AA-Bn] = 20 : 20 : *n*, with n equal to 1, 2, 4, 8). The mixture was condensed at 200 °C for 15 minutes and then incubated at 140 °C until the stir bar speed reached 60 rpm. The polycondensation process was flushed under nitrogen gas and the reaction was stopped by incubating in an ice bath for 10 minutes. The raw POCA prepolymers were dissolved in 100% ethanol and purified by deionized (DI) water precipitation. Lyophilized prepolymers were dissolved in methanol (10%, w/v) and placed under $H_2$ at 4 atm to perform a palladium/carbon-catalyzed hydrogenation reaction to cleave benzyl ethers. The deprotected POCA prepolymer solution was filtered using a Celite pad and centrifuged at 20 000*g* for 60 minutes to remove catalyst. The deprotected POCA prepolymers were evaporated under vacuum for at least 3 days to completely remove any residual amounts of solvent. Prepolymer compositions were characterized by NMR spectra using an INOVA 400 MHz (Varian; Palo Alto, CA, USA), by ultraviolet-visible spectra (UV-vis) on a Cytation 5 plate reader (Biotek; Winooski, VT, USA), by gel permeation chromatography (GPC) on Viscotek VE-2001 system (Malvern Panalytical; Westborough, MA, USA), and by high-resolution mass spectrometry using a Q Exactive HF-X mass spectrometer (ThermoFisher Scientific; Waltham, MA, USA). The relative antioxidant potency of ascorbate in the prepolymers was characterized by an ascorbic acid colorimetric assay kit (catalog #: K661, BioVision; Milpitas, CA, USA). In brief, POCA

prepolymers were dissolved in the dimethyl sulfoxide (DMSO) to determine prepolymer ascorbate activity following the manufacturer's instructions. All values were determined as relative antioxidant potency of ascorbate by comparing with a free ascorbic acid standard curve. NMR and X-ray photoelectron spectroscopy (XPS) on AXIS Nova surface analysis spectrometer (Kratos Analytical Limited; Spring Valley, NY, USA) were used to estimate benzyl residues and palladium/carbon in POCA prepolymers and elastomers.

### 2.2 Elastomer preparation and characterization

**2.2.1 Elastomer preparation.** POC or POCA prepolymers were dissolved in 100% ethanol and poured into round PTFE molds (diameter 3 cm) for solvent evaporation. The POC or POCA prepolymers were evaporated for at least 3 days to completely remove solvent and cured at 80 °C in nitrogen gas for 4 days to prepare corresponding elastomers. POCA elastomer was rinsed by 1× phosphate buffered saline (1× PBS) for 3 days to leach and neutralize the unreacted POCA oligomers for the tests described below.

**2.2.2 Elastomer mechanical testing.** POC or POCA elastomer tensile testing was recorded by a dynamic mechanical analysis (DMA) instrument (RSA-G2, TA Instruments; New Castle, DE, USA) equipped with a displacement model (tension) according to the American Society for Testing and Materials (ASTM) standard 412A. POC or POCA elastomer films were cut into dumbbell shapes (12 mm long × 2 mm wide). The dumbbell-shaped samples were pulled at 0.1 mm $s^{-1}$ and stretched until rupture occurred to measure the strain-at-break ($\varepsilon_{max} = (L_{max} - L_0)/L_0$), where $L_{max}$ is the maximum sample length at break and $L_0$ is the initial sample length. The cross-linking density ($\nu$) and molecular weight between cross-link sites ($M_c$) were evaluated from the Young's modulus ($E \cong \nu RT \cong \rho RT/M_c$)[30] measured as a stress–strain slope at zero strain, where $R$ is the universal gas constant; $T$ is the absolute temperature; $\rho$ is the elastomer mass density.

**2.2.3 Elastomer density, ATR-FTIR and contact angle testing.** POC or POCA elastomer density was measured by a liquid (ethanol) displacement method. POC or POCA elastomer infrared spectra were recorded on a Bruker FTIR (Billerica, MA, USA) with transmission mode and attenuated total reflectance (ATR) mode. POC or POCA elastomer static water contact angle was recorded on a contact angle goniometer (Ramé-Hart; Succasunna, NJ, USA) with DI water dropped onto elastomer surface for 5 minutes.

**2.2.4 Elastomer hydrolytic and ascorbate releasing.** POC or POCA circle discs (diameter 1 cm) were incubated in 1× PBS for monitoring mass loss and ascorbate release. Discs were weighed after samples were lyophilized and the percentage of elastomer mass remaining was determined over 12 weeks by $w_t/w_0 \times 100\%$, where $w_0$ is the initial disc weight and $w_t$ is the lyophilized disc weight. Ascorbate in the hydrolytic degradation product was monitored by the ascorbic acid colorimetric assay kit (BioVision) within 8 weeks. In brief, discs were incubated in 1× PBS at 37 °C and 20 μL of supernatant was collected to determine the ascorbate activity of the hydrolytic degradation products. All values of relative antioxidant potency of ascorbate were determined by comparing with a free ascorbic acid-based standard curve.

### 2.3 Antioxidant activity, *S*-nitrosoglutathione decomposition, and platelet adhesion

**2.3.1 POC- or POCA-coated 48-well plate preparation.** POC or POCA prepolymer solution (100 μL, 15% w/v in ethanol) was used to coat 48-well tissue culture plates (Falcon, Corning; Durham, NC, USA). POC or POCA prepolymers were passed through a sterile syringe filter (PTFE membrane with 0.2 μm pore size, Nalgene; ThermoFisher Scientific; Waltham, MA, USA) before coating onto plates. The prepolymer coated plates were completely evaporated under vacuum and cured at 80 °C in nitrogen gas for 4 days. The plates were fully rinsed by 1× PBS (sterile-filtered) at 37 °C for 3 days and washed by DI water for antioxidant activity, *S*-nitrosoglutathione (GSNO) decomposition, platelet adhesion, and human vascular cell biocompatibility tests (described below).

**2.3.2 POCA elastomer surface ascorbate activity.** The relative antioxidant potency of ascorbate on the elastomer surface was determined by the ascorbic acid colorimetric kit (BioVision) on POCA-coated 48-well plates. The detection kit principle is based on an enzymatic catalyst reaction where an ascorbate colorimetric probe specifically reacts with ascorbic acid to quantitatively determine the ascorbate amount. Following the manufacturer's protocols, we assume that ascorbate colorimetric probes can react with the ascorbate immobilized on the POCA-coated 48-well plate surface and be used to determine ascorbate surface density. All determined values were calculated relative to a free ascorbic acid-based standard curve.

**2.3.3 DPPH (2,2-diphenyl-1-picrylhydrazyl) radical scavenging assay.** The completely rinsed POCA-coated 48-well plates were used to determine DPPH free radical scavenging performance. DPPH stock (600 μM) was prepared in 100% ethanol and was added to elastomer coated 48-well plates to assess free radical scavenging. The plate was incubated at 37 °C and 50 μL of the supernatants was collected at 5, 20, and 40 minutes and monitored by absorbance at 517 nm. DPPH inhibition percentage (%) was calculated as $(1 - A_{sample}/A_{ctrl,\ t=0}) \times 100\%$, where $A_{sample}$ is non-reacted DPPH solution at time $t$ and $A_{ctrl,\ t=0}$ is total non-reacted DPPH solution at time $t = 0$.

**2.3.4 Lipid peroxide inhibition assay.** The completely rinsed polymer-coated 48-well plates were used to determine lipid peroxide inhibition performance. In brief, β-carotene (4 mg), linoleic acid (0.5 mL), and Tween 40 (4 g) were dissolved in chloroform. The chloroform was removed by rotary evaporation and the pre-warmed Britton buffer (30 mL) was added to the oily residue with vigorous shaking. The homogenous mixture was added to POC- or POCA-coated 48-well plates incubated at 45 °C, and the supernatants were collected at 2 hours and 13 hours. The absorbance of the supernatants at 470 nm was used to monitor the ability of polymer-coated 48-well plates to inhibit lipid peroxidation.

**2.3.5 GSNO decomposition assay.** The completely rinsed polymer-coated 48-well plates were used to determine the

 

ability of POC and POCA to decompose GSNO. GSNO solution (0.5 mL 1× PBS containing 0.5 mM EDTA at pH 7.4) was incubated in polymer-coated 48-well plates. Supernatants (10 μL) were collected at different time points within 5 days and diluted 10-fold (by volume) to monitor variations in GSNO concentration. A modified $Hg^{2+}$-based colorimetric Griess assay was used to determine GSNO concentration.[30] In brief, 75 μL of each sample was mixed with 65 μL $HgCl_2$ solution (0.1 mM) and 10 μL Griess reagent at room temperature in a dark environment for 10 minutes. Absorbance of the mixture was then measured at 548 nm and all determined values were calculated *versus* a GSNO standard curve.

**2.3.6 LDH-based platelet adhesion assay.** The completely rinsed polymer-coated 48-well plates were evaluated by *in vitro* platelet adhesion with guinea pig platelet rich plasma (PRP) as previously described, with some modifications.[28] Briefly, PRP was collected from female Hartley guinea pigs in tubes containing anticoagulant citrate dextrose solution (ACD). PRP was isolated by centrifugation at 200*g* for 15 minutes at room temperature and platelet poor plasma (PPP) was isolated by centrifugation of PRP at 850*g* for 20 minutes at room temperature. For testing, the PRP was diluted to $1 \times 10^8$ cells per mL using PPP. Diluted PRP suspension (200 μL) was added to POC- or POCA-coated 48-well plates and incubated at 37 °C for 1 hour. At the end of the platelet adhesion step, the non-adherent platelets were collected and the plate was rinsed three times using 200 μL 1× PBS to collect any remaining non-adherent platelets. These non-adherent platelets were collected, diluted, and quantified using a lactate dehydrogenase (LDH) assay (Cytotoxicity Detection Kit, Roche; Indianapolis, IN, USA) to determine the platelet adhesion rate by measuring absorbance at 490 nm. All LDH values were calculated by a standard curve determined from a known number of platelets counted using a hemocytometer.

### 2.4 Human vascular cell viability and proliferation

The completely rinsed polymer-coated 48-well plates were used to evaluate the biocompatibility of POC and POCA with human vascular cells. Prior to seeding, coated 48-well plates were pre-treated with corresponding cell culture media (smooth muscle cell basal medium and endothelial cell basal medium) until the color of the media did not change. Human aortic smooth muscle cells (HASMC) and human aortic endothelial cells (HAEC) purchased from Lonza (Benecia, CA, USA) were seeded on plates with corresponding basal medium containing growth factors (SmBM/SmGM-2 bullet Kit, and EBM2/EGM2 bullet Kit). Two hundred μL of HASMC and HAEC were seeded at 5000 cells per $cm^2$ (4750 cells per well, well area is 0.95 $cm^2$) and cells of passage 4 to 8 were used for all experiments. HASMC and HAEC viability was evaluated by Live/Dead Viability/Cytotoxicity Kit (ThermoFisher) and proliferation was evaluated by PicoGreen Kit (ThermoFisher) after 1, 3, and 5 days of cell culture. All PicoGreen Kit values were calculated from a standard curve using a known number of HASMC or HAEC counted by a hemocytometer.

### 2.5 Spin-coating of POC- or POCA-ePTFE grafts

**2.5.1 POC- or POCA-ePTFE graft fabrication.** POC- or POCA-ePTFE grafts were prepared by physically covering the node-fibril structure of ePTFE grafts with POC or POCA prepolymer through a modified spin-shearing method.[23] In brief, gas-sterilized ePTFE graft (1.53 mm inner diameter, 100 μm wall thickness and 25 μm internodal distance, Zeus Inc.; Orangeburg, SC, USA) was concentrically placed over a sterile blunt steel needle (18 G and 1.5″, SAI Infusion Technologies; Lake Villa, IL, USA) and the blunt needle was inserted into the motor of a mechanical stirrer (Eurostar 60 control Package, IKA; Wilmington, NC, USA). The POC or POCA prepolymers (15% w/v in ethanol) were passed through a sterile syringe filter (PTFE membrane with 0.2 μm pore size, Nalgene; ThermoFisher Scientific; Waltham, MA, USA). The blunt needle was spun clockwise at 300 rpm and POC or POCA prepolymer was added drop by drop to the top of the graft. The POC or POCA prepolymer fluidly permeated the whole graft through the spinning needle, and the prepolymer layer homogenously covered the luminal surface of ePTFE graft after evaporation. The lumen of the graft was sheared against the blunt needle for 2 minutes by rotating the graft clockwise and counterclockwise to obtain prepolymer-coated ePTFE grafts. This coating procedure was repeated several times to prepare POC- or POCA-ePTFE grafts with the desired mechanical properties. After completely evaporating the residual alcohol in a vacuum drying oven, the ePTFE or prepolymer-coated ePTFE grafts were cured at 80 °C in nitrogen gas for 4 days. The obtained ePTFE, POC-, or POCA-ePTFE grafts were rinsed with 70% ethanol (3×) and incubated in 1× PBS (sterile-filtered) for 3 days for acid leaching. All the ePTFE, POC-, or POCA-ePTFE grafts were rinsed with sterile saline before surgery.

**2.5.2 Elastomer-ePTFE graft mechanical testing.** POC- or POCA-ePTFE graft mechanical properties were tested by DMA and recorded under a displacement model (compression). Briefly, uncoated ePTFE grafts and POC- or POCA-ePTFE grafts were loaded between the DMA parallel plate and force *versus* corresponding displacement were measured in a range of 0 to 1.2 mm with a compression rate at 0.05 mm per second. The compression data were analyzed by a numerical simulation method[38] to qualitatively evaluate the elastic modulus of uncoated ePTFE and POC- or POCA-ePTFE grafts.

### 2.6 Guinea pig aortic interposition graft model

**2.6.1 Animal surgery.** All animal procedures were performed in accordance with the *Guide for the Care and Use of Laboratory Animals* published by the National Institutes of Health and approved by the University of North Carolina at Chapel Hill Animal Care and Use Committee. An aortic interposition graft model was performed on 9 adult (10 to 12 weeks old, 400 to 500 g) female Hartley guinea pigs (GP) as previously described.[39] In brief, GP were anesthetized with inhaled isoflurane (1.5 to 5%) and treated with carprofen subcutaneously for pain control. Surgery was performed using a Wild M650 operating microscope. After a midline incision, an approxi-

mately 1 cm portion of the aorta was removed and the graft was implanted. The proximal and distal anastomoses were fashioned utilizing 10–0 nylon suture *via* 10–13 interrupted sutures. Once hemostasis was achieved, the abdominal cavity and skin were closed in 2 layers using running 4–0 vicryl and running 4–0 nylon suture, respectively. Groups included uncoated ePTFE and POC- or POCA-ePTFE grafts. Guinea pigs were anesthetized at 4 weeks and euthanized *via* bilateral thoracotomies.

**2.6.2 Tissue processing.** Guinea pigs were sacrificed at 4 weeks by exsanguination and bilateral thoracotomies under inhaled anesthesia (isoflurane). This was followed by *in situ* perfusion-fixation through the left ventricle with 1× PBS (300 mL) followed by 2% paraformaldehyde (300 mL). The grafts and adjacent 1 cm of aorta were harvested, cryopreserved in 30% sucrose, and then frozen in liquid nitrogen and stored at −80 °C until sectioning. Samples were cut into 6 μm sections using a CryoStar NX70 Cryostat (ThermoFisher Scientific) and qualitatively studied for neointimal hyperplasia by hematoxylin and eosin (H&E) staining the cross-sections at different levels throughout the harvested graft and tissue. Digital images were obtained using the 2.5× and 20× objectives on an Axio Imager.A2 microscope (Zeiss; Hallbergmoos, Germany) and Axiovision software (release 4.8.2, 06-2010; Pleasanton, CA, USA).

## 3. Results

### 3.1 POCA prepolymer preparation and characterization

POCA prepolymer was prepared following a two-step reaction (Scheme 1A): (i) benzyl-protected POCA prepolymer was prepared *via* combination with citric acid and 1,8-octanediol, which served as the basis for condensing a series of 2,3-benzyl-ascorbate molecules; (ii) POCA prepolymers with enhanced ascorbate activity were prepared by completely removing the benzyl ether *via* hydrogenation. The temperature of initial condensation was optimized from 165 °C to 200 °C to improve benzyl-ascorbate conjugate yield (Table 1) and qualitatively studied by a previously reported method.[30] To investigate the effects of mole feeding ratio, a material map (Fig. 1A) was used to examine actual ascorbate activity (determined by ascorbate kit) in POCA prepolymers *versus* theoretical activity. All synthesized POCA prepolymers exhibited at least 95% ascorbate activity except one (POCA@20 : 20 : 12). This indicated that the mole ratio of carboxyl to hydroxyl groups (Table 1) in the polycondensation reaction determined the successful preparation of POCA prepolymer. It should also be noted that while all POCA prepolymers with [citrate] : [diol] fixed at 20 : 16 can be synthesized, they cannot be cured into solid states with elastic properties. On the other hand, only certain ratios of POCA prepolymers with [citrate] : [diol] fixed at 20 : 20 can be synthesized and easily cured into elastomer, as maximum ascorbate loading terminated when the mole feeding ratio reached 20 : 20 : 8 (Table S1†). Additionally, NMR (Fig. 1B) and UV spectra (Fig. 1C) were tested to assess if POCA prepolymer

**Table 1** POCA prepolymers prepared @200 °C/140 °C

| [CA] : [diol] : [AA] | [–COOH] : [–OH] | Ascorbate conjugating percentage (%) |
|---|---|---|
| 20 : 20 : 1 | 15 : 16 | 90.4 ± 1.2 |
| 20 : 20 : 2 | 15 : 17 | 89.6 ± 0.6 |
| 20 : 20 : 4 | 15 : 19 | 83.8 ± 1.5 |
| 20 : 20 : 8 | 15 : 23 | 72.5 ± 2.5 |

Ascorbate conjugating percentage in prepolymer is calculated as previously reported.[30]

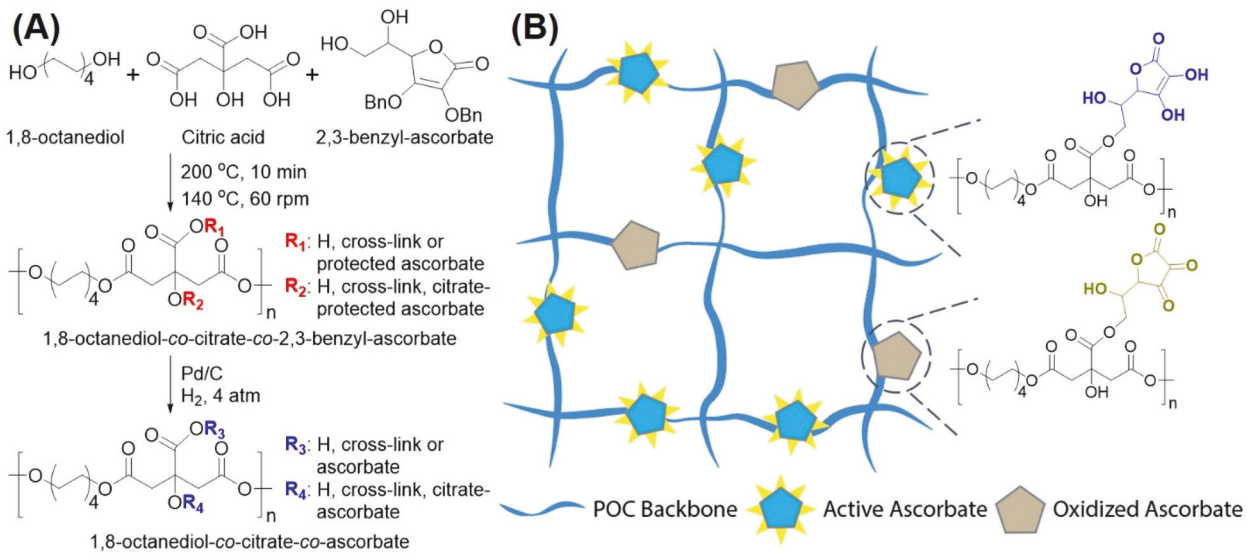


**Scheme 1** (A) Reaction scheme of a two-step synthesis route for POCA prepolymer preparation. (B) Proposed structure of POCA elastomer generated by thermal cross-linking from POCA prepolymer.

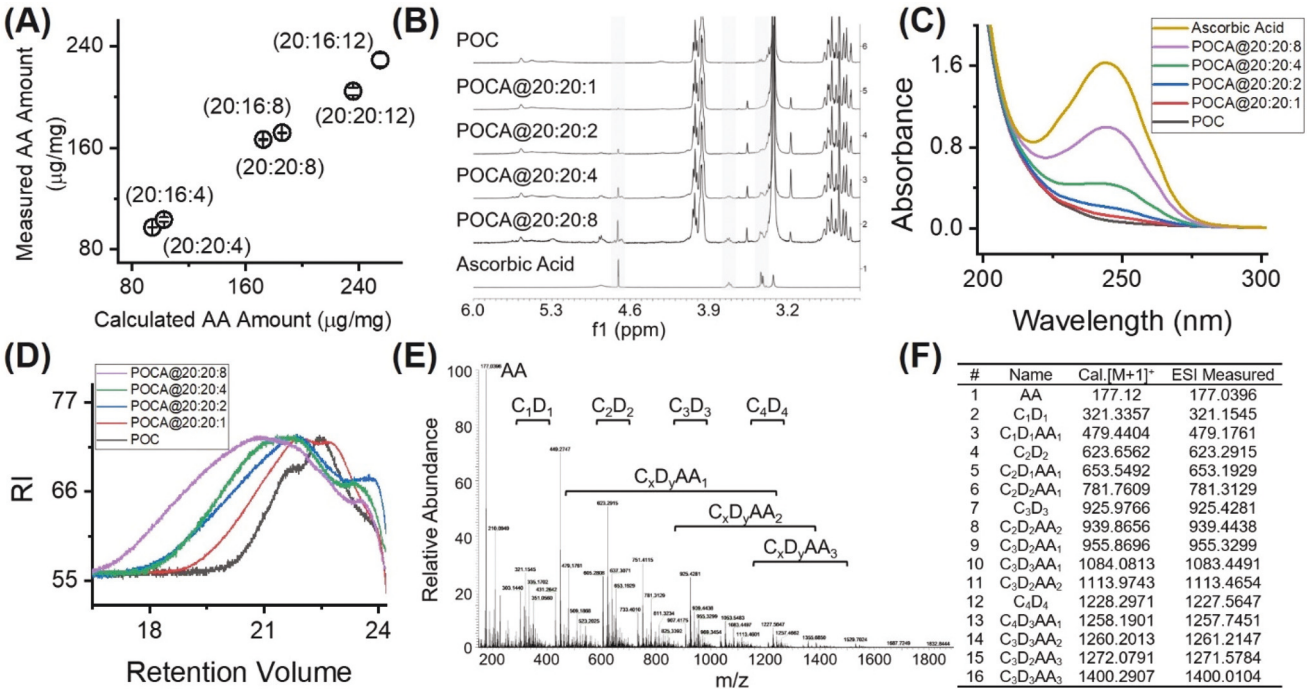


| # | Name | Cal.[M+1]$^+$ | ESI Measured |
|---|---|---|---|
| 1 | AA | 177.12 | 177.0396 |
| 2 | $C_1D_1$ | 321.3357 | 321.1545 |
| 3 | $C_1D_1AA_1$ | 479.4404 | 479.1761 |
| 4 | $C_2D_2$ | 623.6562 | 623.2915 |
| 5 | $C_2D_1AA_1$ | 653.5492 | 653.1929 |
| 6 | $C_2D_2AA_1$ | 781.7609 | 781.3129 |
| 7 | $C_3D_3$ | 925.9766 | 925.4281 |
| 8 | $C_2D_2AA_2$ | 939.8656 | 939.4438 |
| 9 | $C_3D_2AA_1$ | 955.8696 | 955.3299 |
| 10 | $C_3D_3AA_1$ | 1084.0813 | 1083.4491 |
| 11 | $C_3D_2AA_2$ | 1113.9743 | 1113.4654 |
| 12 | $C_4D_4$ | 1228.2971 | 1227.5647 |
| 13 | $C_4D_3AA_1$ | 1258.1901 | 1257.7451 |
| 14 | $C_3D_3AA_2$ | 1260.2013 | 1261.2147 |
| 15 | $C_3D_2AA_3$ | 1272.0791 | 1271.5784 |
| 16 | $C_3D_3AA_3$ | 1400.2907 | 1400.0104 |

**Fig. 1** Characterization of POCA prepolymers. (A) Material map comparing POCA prepolymer theoretical ascorbate *versus* actual ascorbate content. (B) NMR spectra and (C) UV-vis spectra demonstrate increasing trend in ascorbate level. (D) GPC, (E) mass spectra of POCA prepolymer (@20 : 20 : 8, [citrate] : [diol] : [ascorbate]), and (F) table of identified oligomers to verify detailed components of POCA prepolymer (@20 : 20 : 8, [citrate] : [diol] : [ascorbate]).

ascorbate levels are proportional to the ascorbate portion in the feeding ratio. We observed that the higher NMR integrated intensity of protons at ascorbate $C_4$, $C_5$, and $C_6$ (Fig. S1† and Fig. 1B), the more ascorbate portion was involved. A similar trend was also observed on UV-vis spectra by absorbance at 240 nm ($\pi$ to $\pi^*$ excitation of ascorbate C=C bond) in the presence of different mole feeding ratios. These two results indicated that POCA prepolymer ascorbate level can be tuned by mole feeding ratio over the range of 20 : 20 : 1 to 20 : 20 : 8.

POCA prepolymers were tested by GPC for molecular weight and distribution (Fig. 1D) in the presence of different mole feeding ratios (20 : 20 : 1, 20 : 20 : 2, 20 : 20 : 4, and 20 : 20 : 8). The corresponding POCA prepolymer number-average molecular weights ($M_n$) were 1603, 1234, 1018, and 1649 g mol$^{-1}$, and the weight-average molecular weights ($M_w$) were 3469, 2347, 2788, and 5542 g mol$^{-1}$, with a polydispersity (PD) of 2.16, 1.91, 2.74, and 3.36, respectively. The detailed components of POCA prepolymer (@20 : 20 : 8, [citrate] : [diol] : [ascorbate]) were analyzed by ESI-MS spectra (Fig. 1E and F). A strong ascorbate peak at 177.04 *m*/*z* was found by comparing with POC spectra. The molecular-mass difference between the cluster of peaks for 128 *m*/*z* (diol), 174 *m*/*z* (citrate), and 158 *m*/*z* (ascorbate) can be easily identified (Fig. 1F). The citrate-induced cyclic oligomers ($C_xD_x$, $x$ = 2 to 4) with 18 *m*/*z* difference were also identified by comparing with linear ones (Fig. 1E). All the evidence was in good agreement with previously reported MS spectra[28,40] and indicated that POCA prepolymers have a low-molecular mass, as most of the ascorbate was covalently conjugated to the POCA prepolymer polymeric network.

### 3.2 POCA elastomer mechanical properties

POC and POCA elastomers (Scheme 1B) cured from POC and POCA prepolymers were studied through tensile testing to explore their mechanical properties. Cyclic tensile testing of POC and POCA (@20 : 20 : 8, [citrate] : [diol] : [ascorbate]) verified their known elastomeric properties (Fig. S2†). All POCA elastomers exhibited a typical elastomer stress–strain curve (Fig. 2A) without plastic deformation. Young's modulus (2.92 to 5.92 MPa) (Fig. 2B) and ultimate tensile strength (1.53 to 2.91 MPa) (Fig. 2D) increased as POCA elastomer ascorbate level increased, while the consequential strain at break (211.9 to 157.1%) (Fig. 2C) was inversely proportional to increasing POCA elastomer ascorbate level. Using the Young's modulus equation ($E \cong \nu RT \cong \rho RT/M_c$), we calculated that the higher the POCA elastomer ascorbate level, the more dramatically $\nu$ and $M_c$ values increased (Table 2). Additionally, the POCA elastomer final product had a yellow-tinged color, indicating that ascorbate was involved in the polycondensation reaction and may have partially lost activity during the POCA elastomer curing process.

### 3.3 POCA degradation and ascorbate release profile

POCA elastomer degradation (Fig. 3A) was assessed in 1× PBS at 37 °C for 12 weeks. The POCA elastomer discs lost structural integrity by 6 to 8 weeks as the percentage of original mass remaining approached 70 to 80%. It can be seen that the

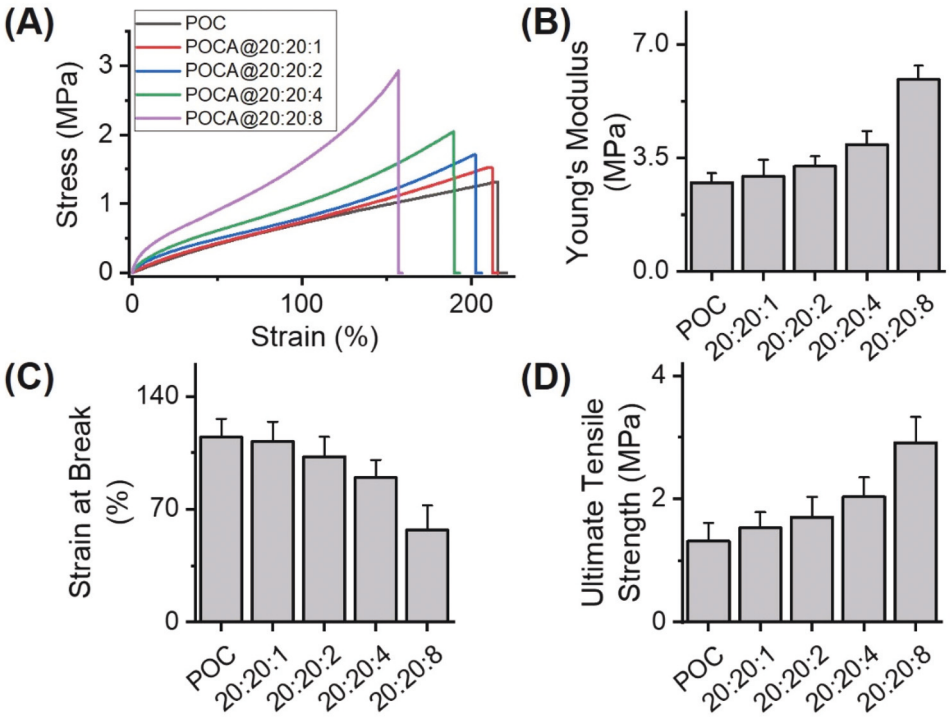


**Fig. 2** Mechanical properties of tunable POCA elastomers. (A) Stress–strain curves, (B) Young's modulus, (C) strain at break, and (D) ultimate tensile strength.

**Table 2** Elastomer physicochemical properties

| [CA] : [diol] : [AA] | $\rho$ (g cm$^{-3}$) | Surface ascorbate density (ng mg$^{-1}$ cm$^{-2}$) | $\nu$ (mol m$^{-3}$) | $M_c$ (g mole$^{-1}$) |
|---|---|---|---|---|
| 20 : 20 : 0 | 1.41 ± 0.05 | N/A | 368 ± 22 | 3838 ± 202 |
| 20 : 20 : 1 | 1.44 ± 0.04 | 4.5 ± 2.5 | 394 ± 26 | 3666 ± 327 |
| 20 : 20 : 2 | 1.49 ± 0.05 | 16.4 ± 3.8 | 436 ± 19 | 3418 ± 276 |
| 20 : 20 : 4 | 1.55 ± 0.11 | 31.9 ± 4.2 | 527 ± 11 | 2947 ± 177 |
| 20 : 20 : 8 | 1.69 ± 0.13 | 67.5 ± 7.3 | 797 ± 21 | 2122 ± 222 |

$\rho$ is elastomer density; $\nu$ is the molar cross-link density calculated as $\nu = E/RT$; $M_c$ is molecular weight between cross-link sites calculated as $M_c = \rho RT/E$.

higher the POCA elastomer ascorbate level, the faster the hydrolytic degradation rate, indicating that ascorbate destabilized the POCA elastomer dependent on the mole feeding ratio. Mass loss studies of POC and POCA elastomers (@20 : 20 : 1, 20 : 20 : 2, 20 : 20 : 4, 20 : 20 : 8) in 100% ethanol showed ~3% mass loss on the 1st day and ~7% mass loss on the 7th day (Fig. S3†). Considering that POCA elastomer degradation products with ascorbate activity might influence vascular cell response, the ascorbate colorimetric kit was used to characterize POCA degradation products by monitoring ascorbate activity for 8 weeks (Fig. 3B). POCA elastomers made using varying mole feeding ratios appeared to continually release degradation products with active ascorbate for more than 2 to 4 weeks. We also noted that the higher the POCA elastomer ascorbate level, the longer and higher the degradation products displayed ascorbate activity.

### 3.4 Characterization of POCA elastomer surface properties

To verify the presence of ascorbate in the POCA elastomer polymeric structure, ATR-FTIR was used to analyze the typical ascorbate C=C stretch (1650 cm$^{-1}$) and the polyester C=O stretch (1730 cm$^{-1}$) from the POCA elastomer. Though IR spectra show little difference between each elastomer, we observed merging of the ascorbate C=C ring stretch and POCA elastomer C=O stretch into an overlapping peak which exhibited a high intensity with a broader peak width trend as the POCA elastomer ascorbate level increased (Fig. 4A). POCA elastomer ascorbate surface density measured by ascorbate kit ranged from 4.5 to 67.5 ng mg$^{-1}$ cm$^{-2}$, as shown in Table 2. With more hydrophilic functional groups (*i.e.*, hydroxyl moiety of ascorbate) exposed to the POCA elastomer surface, the static water-in-air contact angle of POCA elastomers exhibited a downward trend (59° to 45°) as the POCA elastomer ascorbate level increased (Fig. 4B). This trend is similar to the degradation study (Fig. 3A) in that ascorbate appeared to destabilize elastomers with more hydrophilic character. The POCA elastomer (@20 : 20 : 8, [citrate] : [diol] : [ascorbate]) exhibited a smooth surface when imaged by atomic force microscopy (AFM) with a similar roughness value to POC (Fig. S4†). Platelet adherence to foreign surfaces assessed using a lactate dehydrogenase (LDH) assay showed that the surface of POCA elastomers had fewer adherent platelets than the control groups (glass, POC, and TCP), and the number of platelets

 

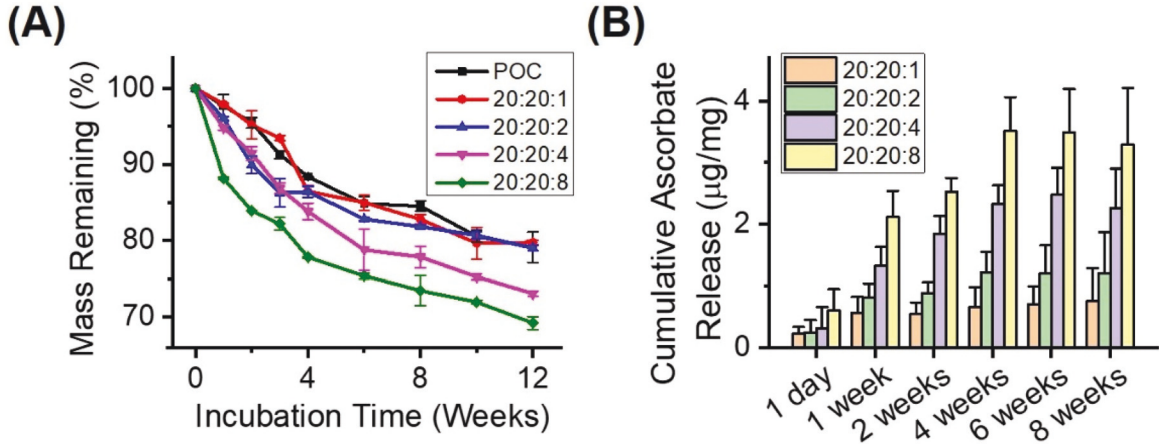


Fig. 3 Degradation properties of tunable POCA elastomers. (A) POCA elastomers undergo hydrolytic degradation in 1× PBS within 12 weeks. (B) POCA elastomer degradation product ascorbate activity over 8 weeks.

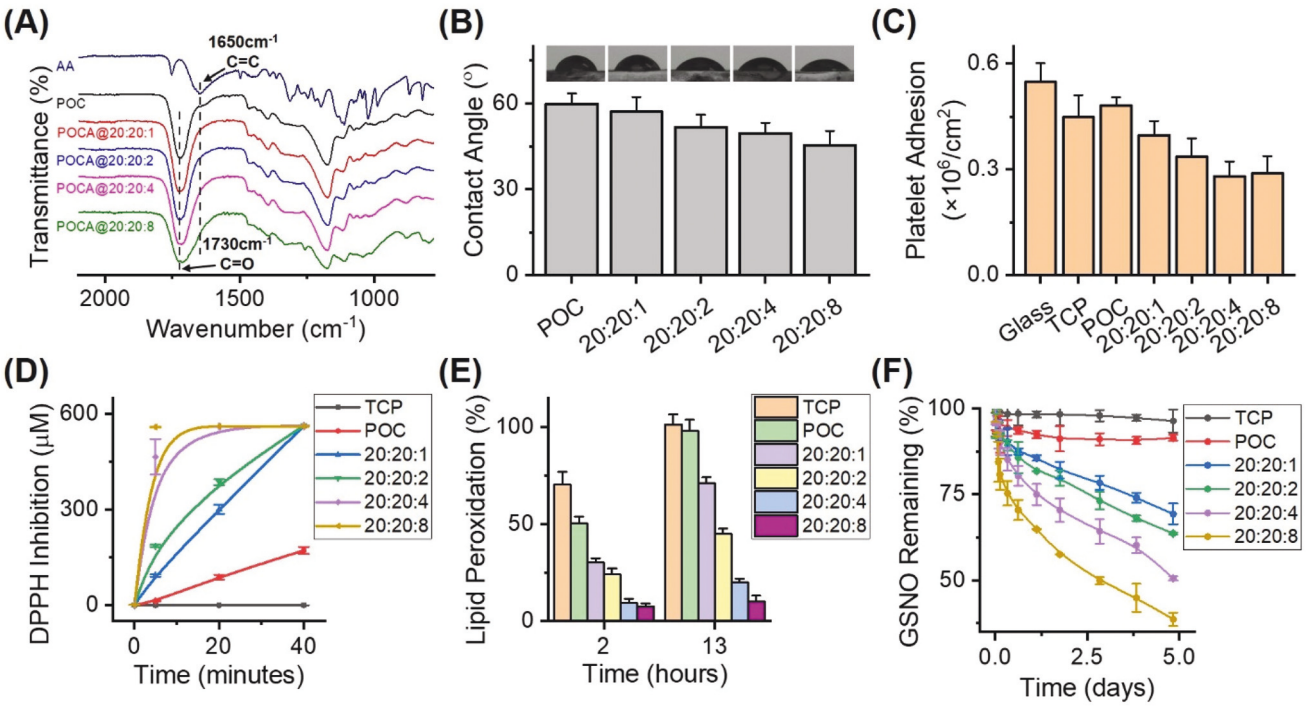


Fig. 4 Surface properties of tunable POCA elastomers. (A) IR spectra of ascorbic acid, POC, and a set of POCA elastomers ([citrate] : [diol] : [AA] = 20 : 20 : 1 to 20 : 20 : 8). (B) Static water-in-air contact angle of POC compared with a set of POCA elastomers. (C) Platelet adhesion on the surface of glass, tissue culture plate (TCP), POC, and a set of POCA elastomers. (D) DPPH free radical inhibition, (E) lipid peroxidation inhibition, and (F) GSNO *in situ* decomposition on the surface of TCP, POC, and a set of POCA elastomers.

decreased as POCA elastomer ascorbate surface density increased (Fig. 4C).

POCA elastomer surface antioxidant activity assessed by DPPH radical scavenging assay showed that, as DPPH-scavenging rate was related with slope of curve at a specific time, POCA elastomer (@20 : 20 : 8, [citrate] : [diol] : [ascorbate]) possessed the highest scavenging response within 40 minutes (Fig. 4D). The scavenging rate increased as the POCA elastomer ascorbate level increased, and the surface DPPH-radical scavenging activity was in the following order: POCA elastomers (20 : 20 : 8 to 20 : 20 : 1) > POC > TCP. Antioxidant performance of POCA elastomer (@20 : 20 : 8, 20 : 20 : 4, 20 : 20 : 2, and 20 : 20 : 1) surface determined by lipid peroxidation inhibition activity was 30.21 ± 2.27, 24.14 ± 2.97, 9.45 ± 2.04, and 7.45 ± 1.57% within 2 hours, and was 71.11 ± 2.98, 45.11 ± 2.55, 20.05 ± 1.82, and 10.11 ± 2.98% within 13 hours, respectively (Fig. 4E). The results indicated that POCA elastomer (@20 : 20 : 8, [citrate] : [diol] : [ascorbate]) has the best inhibi-

tory activity (*i.e.*, higher activity and enhanced durability) than other POCA elastomers (@20 : 20 : 4, 20 : 20 : 2, and 20 : 20 : 1) and control groups (TCP, POC). Moreover, GSNO decomposition assessed using a modified Griess reaction showed that the average scavenging rate on different POCA elastomer surfaces (@20 : 20 : 1, 20 : 20 : 2, 20 : 20 : 4, and 20 : 20 : 8) was 1.05 ± 0.15, 1.23 ± 0.06, 1.46 ± 0.53, and 2.81 ± 0.66 × $10^{-10}$ mol $cm^{-2}$ $min^{-1}$ within 3 hours, and was 0.79 ± 0.05, 0.99 ± 0.02, 1.37 ± 0.17, and 1.92 ± 0.05 × $10^{-10}$ mol $cm^{-2}$ $min^{-1}$ within 8 hours, respectively (Fig. 4F). The results indicated that POCA elastomer (@20 : 20 : 8, [citrate] : [diol] : [ascorbate]) has the best GSNO scavenging activity compared to other POCA elastomers (@20 : 20 : 4, 20 : 20 : 2 and 20 : 20 : 1) and control groups (TCP, POC).

### 3.5 *In vitro* study of POCA elastomer biocompatibility

In order to investigate biocompatibility of tunable POCA elastomers, human aortic smooth muscle cells (HASMC) and human aortic endothelial cells (HAEC) were first assessed on POCA elastomeric thin films in the presence of different ascorbate surface densities. We found that POCA elastomer surfaces with different ascorbate surface densities have antiproliferative and anti-adhesive (Fig. S5†) effects on both HASMC and HAEC (Fig. 5E and F). PicoGreen dsDNA quantification results (Fig. 5C and E) revealed HASMC proliferation was significantly inhibited by POCA surfaces (@20 : 20 : 1 to 20 : 20 : 8) as ascorbate surface density increased (4.5 to 67.5 ng $mg^{-1}$ $cm^{-2}$). HASMC proliferation rate significantly decreased (by 84.6%, $p < 0.001$), especially on POCA elastomer surface (@20 : 20 : 8, [citrate] : [diol] : [ascorbate]) as compared with the POC surface. Live/Dead Cell Viability assay results (Fig. 5A) also revealed that HASMC only covered the POCA-coated plates at 20 to 30% confluence as compared with TCP or POC (90 to 100% confluence after 5 days). Moreover, the HAEC proliferation rate (Fig. 5D and F) significantly decreased (by 49.6%, $p < 0.05$) on POCA elastomer surfaces (@20 : 20 : 8, [citrate] : [diol] : [ascorbate]) as compared with POC. Interestingly, the HAEC proliferation rate did not significantly change as POCA elastomer surface (@20 : 20 : 2, 20 : 20 : 4, and 20 : 20 : 8) ascorbate density significantly increased (16.4 to 67.5 ng $mg^{-1}$ $cm^{-2}$). Live/Dead Cell Viability assay results (Fig. 5B) revealed that HAEC covered the POCA-coated plates at 70 to 80% confluence as compared with TCP or POC (90 to 100% confluence after 5 days). In general, this suggested that HAEC have a more prominent adhesion and proliferation profile than HASMC on POCA elastomer surfaces in the presence of high ascorbate surface density.

### 3.6 Characterization of spin-coated POCA-ePTFE grafts

A simple and facile approach was used to coat the lumen of an ePTFE graft with POCA elastomer (@20 : 20 : 8, [citrate] : [diol] : [ascorbate]) by a modified spin-coating strategy (Fig. S6†).

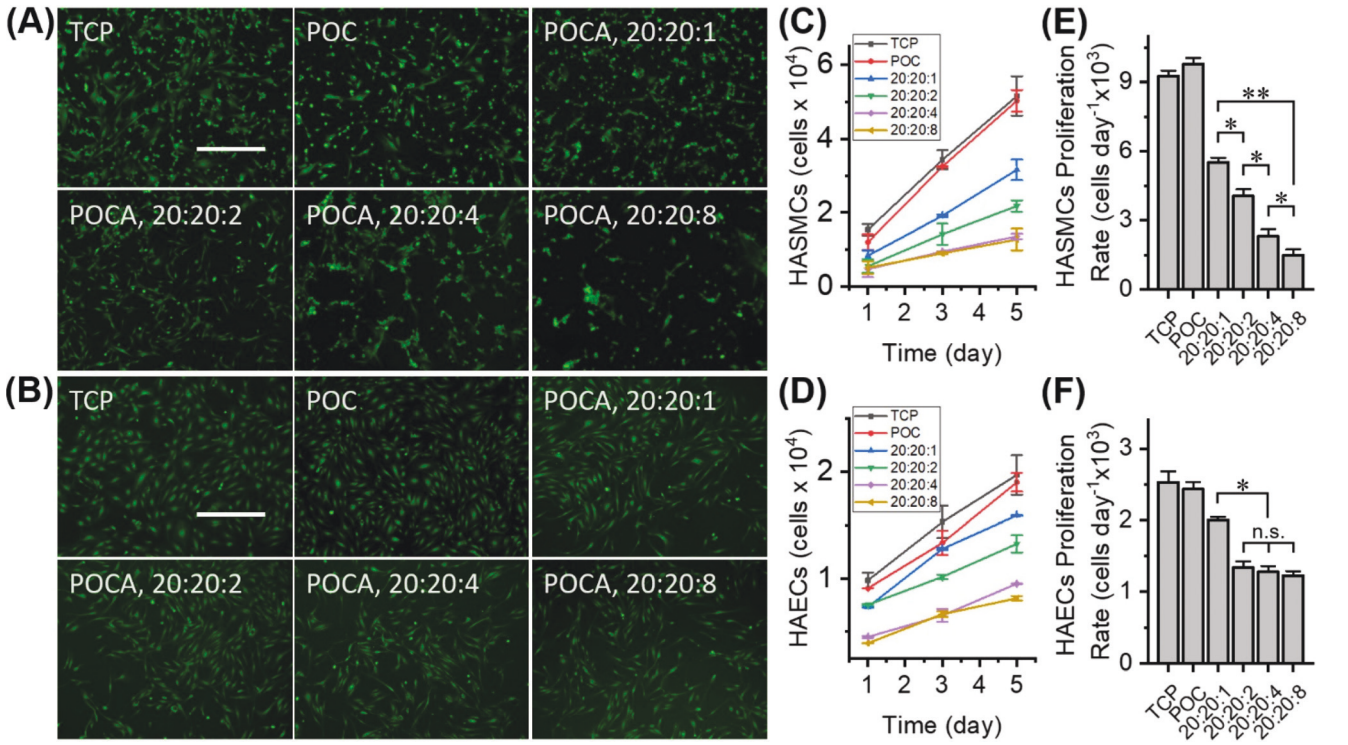


**Fig. 5** HASMC and HAEC viability on TCP surface coated with POC or POCA elastomers over 5 days of cell culture. Fluorescence images of (A) HASMC and (B) HAEC adhesion and viability on TCP, POC, and a set of POCA surfaces ([citrate] : [diol] : [AA] = 20 : 20 : 1 to 20 : 20 : 8) on the 5$^{th}$ day of cell culture. (C and D) Corresponding HASMC and HAEC proliferation profiles on the 1$^{st}$, 3$^{rd}$, and 5$^{th}$ days of cell culture. (E and F) Comparison of HASMC and HAEC proliferation rates over 5 days. Data were analyzed using one-way ANOVA with Bonferroni's *post-hoc* analysis ($n = 5$). *$p < 0.05$. **$p < 0.001$. n.s. is not statistically significant. Scale bar is 400 μm.

SEM imaging was used to monitor lumen graft micromorphology alteration as the number of coatings increased (Fig. 6A). The fibrillary, porous structure of the ePTFE graft lumen was covered and filled by POCA elastomer as the coating number increased. The porous network of the ePTFE graft lumen showed a pore size less than 20 to 30 μm until the 4$^{th}$ spin-coating. The POCA-ePTFE graft fibrillary microstructure appeared completely filled by POCA elastomers after the 7$^{th}$ spin-coating. The corresponding mass and mechanical property alterations were monitored as the number of coatings increased (Fig. 6B and C). The mass of POCA elastomer (@20 : 20 : 8, [citrate] : [diol] : [ascorbate]) coated onto the 2 cm ePTFE graft ranged from 0 to 2.76 mg and the corresponding graft modulus ranged from 2.42 to 7.07 MPa, as estimated by a reported simulation method[38] and shown in Fig. S7.† These data indicate that using a modified spin-coating strategy generated POCA-ePTFE grafts with tunable mechanical properties that will be much more suitable for vascular engineering applications. Future studies will assess POCA-coated ePTFE grafts by elemental analysis, nano indentation, and AFM.

### 3.7 *In vivo* study of the ability of POCA-ePTFE grafts to reduce neointimal hyperplasia

To further examine the ability of POCA elastomer to reduce neointimal hyperplasia *in vivo*, uncoated ePTFE, POC-ePTFE, and POCA-ePTFE grafts were implanted in a guinea pig aortic interposition bypass model. Straight ePTFE grafts 1 cm in length and 1.5 mm in diameter were coated with POC and POCA (@20 : 20 : 8, [citrate] : [diol] : [ascorbate]) elastomer 4 times using our modified spin-coating method. Compression force *vs.* graft length change (Fig. 7A), radial compression forces (Fig. 7B), and corresponding surface micromorphologies (Fig. 7C) of uncoated ePTFE, POC-ePTFE, and POCA-ePTFE grafts showed that there were slight increases in the dimensions and significant changes in the mechanical properties of coated grafts (Table S2†). The grafts were implanted as an interposition end-to-end vascular graft in female guinea pigs (Fig. S8†). Four weeks after implantation, uncoated ePTFE, POC-ePTFE, and POCA-ePTFE grafts were harvested and sectioned. Representative H&E-stained cross-sections taken from the middle of implanted uncoated ePTFE, POC-ePTFE, and POCA-ePTFE grafts (0.5 cm) showed that the POCA-ePTFE graft more effectively reduced neointimal hyperplasia *versus* uncoated ePTFE and POC-ePTFE grafts (Fig. 7C). Lumen area was greatest in POCA-ePTFE and least in ePTFE.

## 4. Discussion

Development of small-diameter prosthetic vascular grafts with clinically acceptable patency rates continues to be a goal of cardiovascular research. Our group's long-term research interest is in synthesizing and characterizing small-diameter ePTFE grafts that provide renewable reservoirs of small molecule therapies at the site of vascular intervention to prevent complications that lead to graft occlusion. We are strongly interested

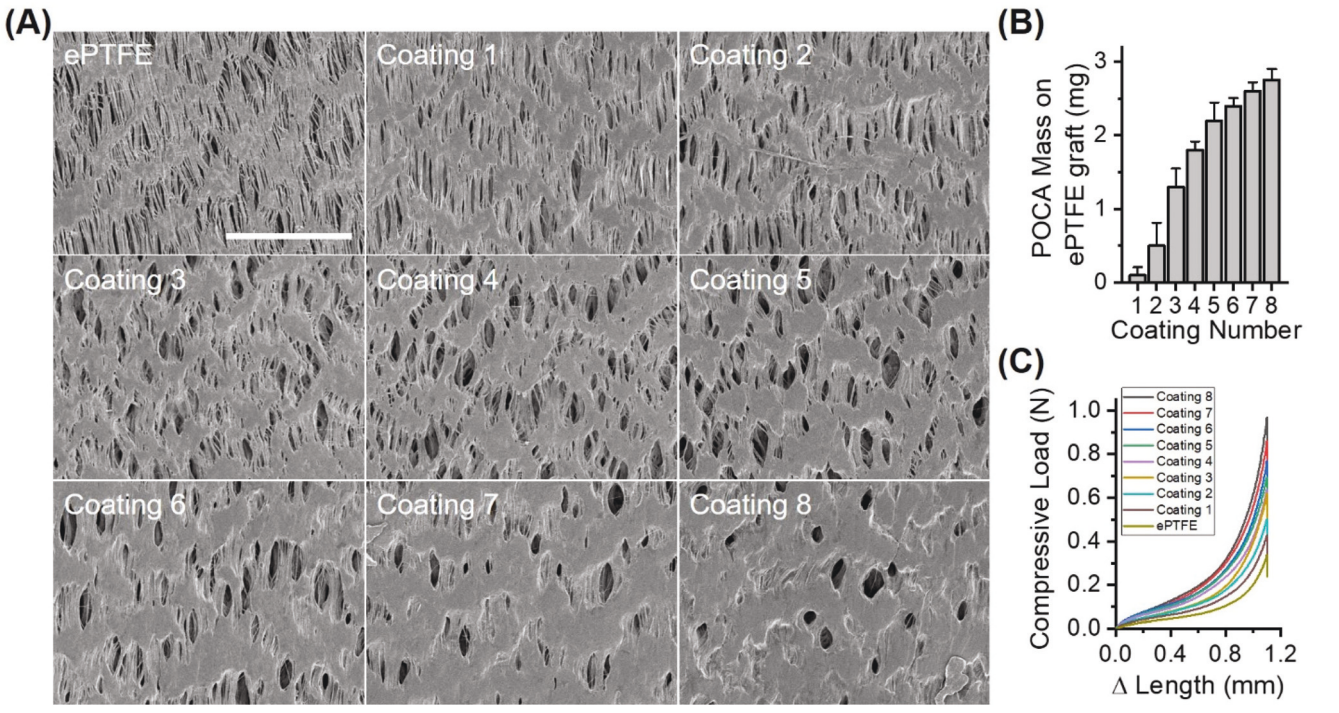


**Fig. 6** Characterization of spin-coating fabrication of POCA-ePTFE grafts (2 cm in length). (A) SEM micrograph of the POCA-coated ePTFE graft lumen surface, (B) measurement of mass of POCA elastomer coated onto grafts, and (C) compression of POCA-ePTFE grafts *versus* coating numbers. Scale bar is 50 μm.

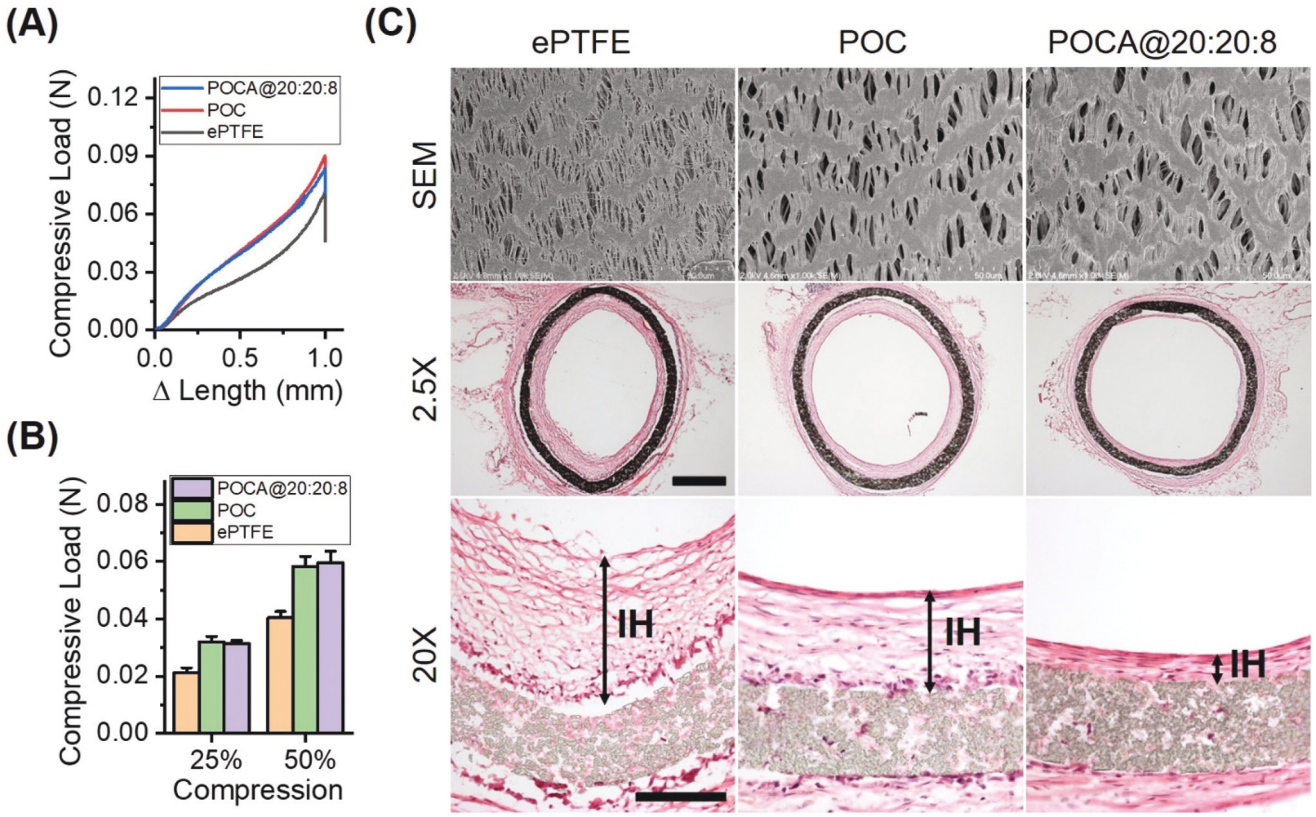


**Fig. 7** Mechanical property comparison and histological analysis of uncoated *versus* coated grafts implanted in a guinea pig interposition model. (A) Radial compression measurements of 1 cm long uncoated ePTFE, POC-ePTFE, and POCA-ePTFE grafts prior to implantation. (B) Force comparison of 1 cm uncoated ePTFE, POC-ePTFE, and POCA-ePTFE grafts at 25 and 50% compression. (C) SEM of the luminal surface of uncoated ePTFE, POC-ePTFE, and POCA-ePTFE grafts show micromorphology prior to implantation. H&E staining of representative graft sections taken from the middle of implanted grafts (0.5 cm) show neointimal hyperplasia (IH, black arrows) at 4 weeks post-implantation (2.5× scale bar = 0.5 mm; 20× scale bar = 70 μm).

in the simplest chemical forms of vitamin C, comprising L-ascorbate and dehydro-L-ascorbic acid, as therapeutic molecules with enormous potential to achieve this goal. We previously developed a POCA elastomer that, when coated on the lumen of an ePTFE graft, inhibited neointimal hyperplasia while maintaining graft compliance.[28] However, the reduction in neointimal hyperplasia was not as robust as it could be, likely due to insufficient ascorbate activity of the POCA elastomer. There is still a vast potential to develop POCA elastomers by an alternative strategy to enhance elastomer ascorbate activity with 2 design criteria: (i) an effective shielding method to protect ascorbate from the harsh prepolymer synthesis conditions; and (ii) a proper mole feed ratio to maximally load ascorbate onto POCA prepolymers and cure them into POCA elastomers. We have recently published a POCA prepolymer preparation method that increases active ascorbate using a protection/deprotection strategy.[30] By tuning the mole feed ratio to achieve maximum ascorbate activity, we can make these prepolymers ideal candidates for curing moldable POCA elastomers.

The mechanism for converting POCA prepolymer to elastomer was to thermally cross-link the carboxylic acid groups and alcohol groups of the polyfunctional POCA prepolymer to tailor a resulting biodegradable elastomer with a controllable number of cross-links.[41] POCA elastomers prepared *via* self-polymerization of prepolymer carboxylic acid groups and hydroxyl groups found on citric acid, 1,8-octanediol, and ascorbate were tuned by adjustment of mole feed ratios to provide a range of values for Young's modulus, strain at break, and ultimate tensile strength. The changing of these indices suggests that the mechanical properties of POCA elastomers depend on the amount of ascorbate they carry. For instance, ascorbate may act as a cross-linking site involved in the polycondensation reaction with the citrate polymer network during the POCA elastomer curing process. To be an ideal elastomer-based biomaterial, POCA needs to have suitable mechanical properties that would be beneficial to tissue engineering, especially for vascular engineering applications.[42] It should be noted that the mechanics of blood vessels are generally viscoelastic and strain-stiffening with an upper modulus region from 2 to 6 MPa.[43] As our 4 present POCA elastomers have a tunable modulus and ultimate tensile strength up to 2 times higher than POC, they are within the same order of magnitude as POC elastomer and have a similar profile to the upper

 

modulus region of blood vessels. Thus, it is likely that coating small-diameter ePTFE grafts with tunable POCA elastomers could reduce vascular complications induced by mismatched mechanical properties of native vessels and prosthetic grafts.[4]

The POCA elastomer degradation and release assay strongly suggested that active ascorbate on the POCA elastomer surface and released POCA degradation products containing active ascorbate comprised the main localized therapeutic moieties of POCA-coated grafts. Active ascorbate plays an important role in modulating SMC and EC responses to implantation of a foreign material, such as activation, immigration, and proliferation.[31,32] Since the citric acid, 1,8-octanediol, and ascorbate monomers that make up POCA are nontoxic natural products, POCA elastomer degradation products are safe, though they have a yellow-tinged color caused by ascorbate oxidation products such as furans, ketoacids, and carboxylic acids.[44] Additionally, the active ascorbate content in bulk POCA elastomers (@20 : 20 : 1, 20 : 20 : 2, 20 : 20 : 4, 20 : 20 : 8) cannot be tested directly, but it can be approximately estimated by the cumulative ascorbate release profile at saturation stage (4 to 6 weeks), for a minimum value of 0.65, 1.21, 2.33, and 3.51 μg $mg^{-1}$, respectively.

Increasing POCA elastomer ascorbate surface density has become an important research avenue in our group. Our current method of preparing POCA prepolymer, which combines our ascorbate protection/deprotection strategy with adjustments to the mole feed ratio, allowed for significant improvements in POCA elastomer ascorbate surface density. For example, our current POCA elastomer (@20 : 20 : 8, [citrate] : [diol] : [ascorbate]) has about 2-fold higher ascorbate surface density than previously reported for POCA elastomer (@5 : 5 : 1),[43] and it has about 4-fold higher ascorbate surface density than previously reported for unprotected POCA elastomer (@5 : 5 : 1).[28] We have also characterized a series of interesting phenomena on POCA elastomer surfaces, including platelet adhesion, antioxidant activity, and GSNO decomposition, which are caused by the enhanced ascorbate surface density of the current POCA elastomer.

A great challenge for blood-contacting medical devices is the risk of thrombosis due to platelet activation and adhesion. Though platelet activation and adhesion is a complex subject, surface wettability, surface functional groups, and surface roughness have been considered important individual factors for biomaterial interface design to decrease platelet adhesion.[45] Given the hydrophilicity and smoothness we demonstrated of the POCA elastomer surface, it appears to be a very suitable coating for blood-contacting materials. The LDH-based platelet adhesion assay indicated that POCA elastomer surfaces have a significantly lower platelet adhesion rate as POCA elastomer ascorbate surface density increased. These data suggest that POCA elastomers coated on the lumen of small-diameter ePTFE grafts have the potential to improve graft hemocompatibility by decreasing platelet adhesion.

Ascorbate is one of the most effective water soluble antioxidants and is deployed in human blood as an endogenous antioxidant to protect tissues and cells from oxidation damage, such as a buildup of oxidized low-density lipoproteins.[46] Ascorbate can donate a hydrogen atom to an oxidizing system to form a relatively stable complex with free radicals and quench superoxide.[47] Since our results suggested that POCA elastomers maintain the intrinsic antioxidant properties of ascorbate, we used DPPH radical scavenging and lipid peroxidation assays to assess the antioxidant activity of POCA elastomers. DPPH radical scavenging activity of POCA elastomer (@20 : 20 : 8, [citrate] : [diol] : [ascorbate]) was higher than other POCAs, with all DPPH-radical scavenged within 20 minutes. Lipid peroxidation inhibition activity of POCA elastomer (@20 : 20 : 8, [citrate] : [diol] : [ascorbate]) was also higher than other POCA elastomers, as only 10.1 ± 2.9% β-carotene was bleached after 13 hours at 45 °C. The ascorbate activity of POCA degradation products also indicated that the ascorbate involved in DPPH radical scavenging and lipid peroxidation inhibition is the portion of ascorbate on the POCA polymeric structure. It should also be noted that, while a portion of ascorbate was oxidized during the elastomer curing process, POCA elastomers still demonstrated ascorbate-based antioxidant activity and capacity commensurate with their ascorbate content.

A polymer surface with the ability to catalyze breakdown of endogenous GSNO and mimic the endogenous nitric oxide (NO) flux rate of endothelial cells is essential for vascular engineering. NO has been recognized as a guardian for vascular grafts and its wide-ranging biological functions have been reported on platelets, SMC, and EC.[48] Ascorbate has been reported to scavenge GSNO through ascorbyl radicals by cleaving the S–N bond *via* nucleophilic attack,[49–51] converting GSNO to a disulfide after transferring NO. Our results indicated that POCA elastomers can scavenge GSNO and release NO with a tuned performance in the presence of different POCA elastomer ascorbate surface densities. For example, the surface of POCA elastomer (@20 : 20 : 8, [citrate] : [diol] : [ascorbate]) showed an average scavenging rate of 2.81 ± 0.66 × $10^{-10}$ mol $cm^{-2}$ $min^{-1}$ within the first 3 hours, which is almost 2-fold higher than NO flux rate of endothelial cells.[48] Moreover, nitroxyl (HNO) can be formed by the reduction of nitric oxide with ascorbate,[52] and our group previously reported that HNO has inhibitory effects on SMC and EC proliferation, leading to moderation of neointimal hyperplasia formation and development *in vivo*.[53] Additionally, the powerful antioxidant performance of the POCA elastomer surface likely provides an effective antioxidant microenvironment to eliminate oxidative stress and protect NO *in situ* from oxidation by a variety of iron proteins found in physiological environments.[54]

As POCA elastomer ascorbate surface density increased, the surfaces of POCA elastomers showed greater anti-adhesive and antiproliferative effects on HASMC *versus* HAEC. Due to the important roles that HASMC and HAEC play in the development of neointimal hyperplasia, POCA elastomers that inhibit HASMC proliferation while maintaining HAEC proliferation will be beneficial for use in vascular engineering applications. Though the mechanism of POCA elastomers inhibiting HASMC and HAEC proliferation is difficult to elucidate, the

physicochemical properties of POCA elastomers such as pro-oxidant activity, adhesion peptide binding strength, and weak acid microenvironment are considered essential factors in biological processes.[55] Moreover, EC seeding density is an important parameter for optimal growth *in vitro* and their proliferation rate is closely correlated to initial cell seeding density. Though the POCA surface displayed anti-adhesive effects on HAEC, their proliferation rate was not significantly decreased as ascorbate surface density significantly increased from 4.5 to 67.5 ng $mg^{-1}$ $cm^{-2}$. This implies that HAEC proliferation is not inhibited by ascorbate surface density and that the surfaces of POCA elastomers will affect HASMC much more than HAEC as ascorbate surface density is increased. Additionally, we observed that HAEC tend to exhibit a more elongated adhesive morphology as the ascorbate surface density of POCA elastomers increased. Previous studies by other groups have indicated that stiffness might play an essential role in modulating the orientation morphology of the endothelium,[56] and that line-shaped endothelial cells will benefit from the formation of confluent endothelium.[57] Our results indicate that a suitable modulus of POCA elastomers can be tuned by controlling ascorbate levels to achieve a stiffness that will protect the endothelium by providing endothelial cells with an *in vivo*-like orientation and strong cell–cell junctions. Future studies will include assessments of the biological influence of the oxidation products of ascorbate.

POCA-ePTFE grafts with tunable physical and mechanical properties are desirable materials for *in vivo* study. Though ePTFE grafts are high modulus isotropic conduits, our results indicate that applying POCA elastomer (@20 : 20 : 8, [citrate] : [diol] : [ascorbate]) *via* spin-coating can provide POCA-ePTFE grafts as elastic as native vessels and with mechanical and porous properties that are tunable by adjusting the number of coatings. The elastomeric characteristics of POCA-ePTFE grafts also likely help prevent changes in hemodynamic forces, such as shear stress and transmural pressure, which are involved in regulating SMC cellular functions such as increased PDGF and PDGF receptor expression, and induction of the MAPK pathway[58,59] that predispose formation of neointimal hyperplasia in implanted grafts.[60] Moreover, the micromorphology of the POCA-ePTFE graft lumen with microporous structure (20 to 30 μm pore size) may promote small-diameter vascular graft re-endothelialization, healing, and incorporation to the surrounding tissue after implantation.[61,62] In sum, facile spin-coating of ePTFE grafts with POCA elastomer (@20 : 20 : 8, [citrate] : [diol] : [ascorbate]) provides prominent aspects that allow for evaluation of the ability of these materials to prevent neointimal hyperplasia *in vivo*.

After assessment of the performance of engineered POCA elastomers and grafts *in vitro*, we implanted POCA-ePTFE grafts in guinea pigs to assess formation of neointimal hyperplasia in an aortic interposition graft model. Due to the multifactorial biological processes that result in the formation of neointimal hyperplasia, 3 criteria were considered when designing POCA-ePTFE grafts for implantation: (i) POCA elastomer (@20 : 20 : 8, [citrate] : [diol] : [ascorbate]) was chosen as the most promising therapeutic candidate for fabrication of POCA-ePTFE grafts due to its enhanced antioxidant, antiplatelet, and antiproliferative effect on SMC; (ii) 4 was the number of spin-coatings determined to maintain the fibrillary, porous microstructure of the ePTFE graft lumen with a pore size of 20 to 30 μm while supporting ePTFE graft shape without significant changes in graft dimensions; and (iii) though the mechanical properties of the POCA-ePTFE graft changed as modulus increased 2-fold, they are still comparable with POC-ePTFE grafts, allowing for assessment of the effects of ascorbate in reducing neointimal hyperplasia. Our previous study showed that small-diameter uncoated ePTFE grafts implanted in a guinea pig model were prone to intimal hyperplasia.[39] Guinea pigs were chosen due to their ability to mimic humans, as both species lack the terminal enzyme that synthesizes ascorbate from glucose (L-gulonolactone oxidase).[63] Female guinea pigs were chosen initially because we previously showed that female rodents regulate oxidative stress differently than male rodents.[64] Ongoing studies will assess the POCA-ePTFE grafts in both sexes. Since our previous studies have shown that the development of neointimal hyperplasia in the proximal and distal segments of uncoated ePTFE grafts is different in a guinea pig model *versus* a rat model,[39] we selected the middle of the graft as a typical cross-section to evaluate the effect of POCA-ePTFE grafts to reduce neointimal hyperplasia. We found that POCA-ePTFE grafts have a remarkable neointimal hyperplasia reduction effect when compared to uncoated ePTFE and POC-ePTFE grafts. This phenomenon may be due to: (i) active ascorbate on the POCA elastomer surface and from degraded oligomers inhibiting SMC activation, migration, and proliferation while maintaining EC cytocompatibility and promoting endothelial healing; (ii) enhanced antioxidant performance of POCA degrading ROS released from activated platelets as well as oxidized low-density lipoproteins (LDL), preventing EC apoptosis induced by oxidized LDL and inhibiting SMC activation, proliferation, and migration induced by ROS or oxidized LDL; and (iii) scavenging of endogenous GSNO by POCA elastomer to enhance *in situ* release of NO in the guinea pig, thus reducing intimal development in the graft lumen.

Currently, there are no effective strategies to prevent neointimal hyperplasia in prosthetic grafts, and there are few studies in recent years employing small-diameter ePTFE graft lumen modification to bind functional biomaterials for *in vivo* inhibition of intimal hyperplasia formation.[65,66] The current study shows that coating a 1.5 mm diameter ePTFE graft with biodegradable and biocompatible POCA elastomers that have tunable mechanical and antioxidant properties significantly decreased intimal area after one month. One limitation of our study is the relatively short time frame over which we assessed neointimal hyperplasia formation. Studying the behavior of an implanted POCA-ePTFE graft over a much longer term (6 months to a year) would establish the feasibility of small-diameter POCA-ePTFE grafts to promote vascular regenerative effects such as EC coverage and SMC inhibition. Another limitation is that we did not use other techniques, such as long-

 

term compliance assessment, to monitor and quantitatively analyze the POCA-ePTFE graft, and to elucidate the relationship between ascorbate, biomechanical factors, and endothelialization. This mechanistic study of the efficacy of POCA-ePTFE grafts at inhibiting intimal formation would be enlightening.

## 5. Conclusion

Neointimal hyperplasia limits the long-term success of small-diameter ePTFE graft interventions. We demonstrated the need to develop POCA elastomers as effective therapeutic biomaterials to modify the luminal surface of small-diameter ePTFE grafts in order to overcome graft occlusion induced by neointimal hyperplasia. Given the *in vitro* and *in vivo* therapeutic effects of POCA elastomer—including antioxidant activity, GSNO decomposition, SMC inhibition, and neointimal hyperplasia reduction—the findings and mechanism elucidated in the present study may be helpful in the development of ascorbate-based surface coatings to inhibit neointimal hyperplasia and maintain long-term patency of small-diameter ePTFE grafts.

## Author contributions

Lu Yu: Conceptualization, methodology, validation, formal analysis, writing – original draft, project administration. Emily R. Newton: Methodology, validation, writing – review & editing. David C. Gillis: Investigation, writing – review & editing. Kui Sun: Investigation, writing – review & editing. Brian C. Cooley: Resources, investigation, writing – review & editing. Andrew N. Keith: Investigation, writing – review & editing. Sergei S. Sheiko: Resources, investigation, writing – review & editing. Nick D. Tsihlis: Conceptualization, methodology, resources, validation, writing – review & editing, project administration, supervision, funding acquisition. Melina R. Kibbe: Conceptualization, methodology, resources, validation, writing – review & editing, project administration, supervision, funding acquisition.

## Conflicts of interest

There are no conflicts to declare.

## Acknowledgements

This material is based upon work supported in part by the Department of Veterans Affairs, Veterans Health Administration, Office of Research and Development and Biomedical Laboratory Research and Development (5I01BX002282 to MRK). The views expressed in this article are those of the authors and do not necessarily reflect the position or policy of the Department of Veterans Affairs or the United States government. SSS and ANK acknowledge funding from the National Science Foundation (DMR 1921835 and DMR 2004048).

## References

1 S. M. Vartanian and M. S. Conte, *Circ. Res.*, 2015, **116**, 1614–1628.
2 A. H. Sepehripour and T. Athanasiou, *Expert Rev. Cardiovasc. Ther.*, 2016, **14**, 367–379.
3 S. S. Virani, A. Alonso, E. J. Benjamin, M. S. Bittencourt, C. W. Callaway, A. P. Carson, A. M. Chamberlain, A. L. R. Chang, S. S. Cheng, F. N. Delling, L. Djousse, M. S. V. Elkind, J. F. Ferguson, M. Fornage, S. S. Khan, B. M. Kissela, K. L. Knutson, T. W. Kwan, D. T. Lackland, T. T. Lewis, J. H. Lichtman, C. T. Longenecker, M. S. Loop, P. L. Lutsey, S. S. Martin, K. Matsushita, A. E. Moran, M. E. Mussolino, A. M. Perak, W. D. Rosamond, G. A. Roth, U. K. A. Sampson, G. M. Satou, E. B. Schroeder, S. T. H. Shah, C. M. Shay, N. L. Spartano, A. Stokes, D. L. Tirschwell, L. B. VanWagner, C. W. Tsao and C. Amer Heart Assoc, *Circulation*, 2020, **141**, E139–E596.
4 W. E. Burkel, *Med. Prog. Technol.*, 1989, **14**, 165–175.
5 H. Ariyoshi, M. Okuyama, K. Okahara, T. Kawasaki, J. Kambayashi, M. Sakon and M. Monden, *Thromb. Res.*, 1997, **88**, 427–433.
6 M. S. Lemson, J. H. M. Tordoir, M. Daemen and P. Kitslaar, *Eur. J. Vasc. Endovasc. Surg.*, 2000, **19**, 336–350.
7 W. Wu, R. A. Allen and Y. D. Wang, *Nat. Med.*, 2012, **18**, 1148–1154.
8 R. A. Allen, W. Wu, M. Y. Yao, D. Dutta, X. J. Duan, T. N. Bachman, H. C. Champion, D. B. Stolz, A. M. Robertson, K. Kim, J. S. Isenberg and Y. D. Wang, *Biomaterials*, 2014, **35**, 165–173.
9 Y. Yang, D. Lei, H. X. Zou, S. X. Huang, Q. Yang, S. Li, F. L. Qing, X. F. Ye, Z. W. You and Q. Zhao, *Acta Biomater.*, 2019, **97**, 321–332.
10 W. H. Gong, D. Lei, S. Li, P. Huang, Q. Qi, Y. J. Sun, Y. J. Zhang, Z. Wang, Z. W. You, X. F. Ye and Q. Zhao, *Biomaterials*, 2016, **76**, 359–370.
11 M. R. Kapadia, D. A. Popowich and M. R. Kibbe, *Circulation*, 2008, **117**, 1873–1882.
12 M. A. Hiob, S. She, L. D. Muiznieks and A. S. Weiss, *ACS Biomater. Sci. Eng.*, 2017, **3**, 712–723.
13 D. Radke, W. K. Jia, D. Sharma, K. Fena, G. F. Wang, J. Goldman and F. Zhao, *Adv. Healthcare Mater.*, 2018, **7**, 1–24.
14 R. A. Hoshi, R. Van Lith, M. C. Jen, J. B. Allen, K. A. Lapidos and G. Ameer, *Biomaterials*, 2013, **34**, 30–41.
15 H. Y. Mi, X. Jing, J. A. Thomsom and L. S. Turng, *J. Mater. Chem. B*, 2018, **6**, 3475–3485.
16 A. Gao, R. Q. Hang, W. Li, W. Zhang, P. H. Li, G. M. Wang, L. Bai, X. F. Yu, H. Y. Wang, L. P. Tong and P. K. Chu, *Biomaterials*, 2017, **140**, 201–211.

17 L. Chen, H. P. He, M. A. Wang, X. X. Li and H. H. Yin, *Tissue Eng. Regener. Med.*, 2017, **14**, 359–370.
18 S. G. Wise, H. J. Liu, A. Kondyurin, M. J. Byrom, P. G. Bannon, G. A. Edwards, A. S. Weiss, S. S. Bao and M. M. Bilek, *ACS Biomater. Sci. Eng.*, 2016, **2**, 1286–1297.
19 F. R. Pu, R. L. Williams, T. K. Markkula and J. A. Hunt, *Biomaterials*, 2002, **23**, 4705–4718.
20 I. Tzchori, M. Falah, D. Shteynberg, D. L. Ashkenazi, Z. Loberman, L. Perry and M. Y. Flugelman, *Mol. Ther.*, 2018, **26**, 1660–1668.
21 A. K. Ranjan, U. Kumar, A. A. Hardikar, P. Poddar, P. D. Nair and A. A. Hardikar, *PLoS One*, 2009, **4**, 1–11.
22 J. Yang, A. R. Webb, S. J. Pickerill, G. Hageman and G. A. Ameer, *Biomaterials*, 2006, **27**, 1889–1898.
23 J. Yang, D. Motlagh, J. B. Allen, A. R. Webb, M. R. Kibbe, O. Aalami, M. Kapadia, T. J. Carroll and G. A. Ameer, *Adv. Mater.*, 2006, **18**, 1493–1498.
24 D. Motlagh, J. Allen, R. Hoshi, J. Yang, K. Lui and G. Ameer, *J. Biomed. Mater. Res., Part A*, 2007, **82**, 907–916.
25 R. T. Tran, J. Yang and G. A. Ameer, in *Annual Review of Materials Research, Vol 45*, ed. D. R. Clarke, Annual Reviews, Palo Alto, 2015, vol. 45, pp. 277–310.
26 C. Y. Ma, E. Gerhard, D. Lu and J. Yang, *Biomaterials*, 2018, **178**, 383–400.
27 E. K. Gregory, A. Webb, J. M. Vercammen, M. E. Kelly, B. Akar, R. van Lith, E. M. Bahnson, W. L. Jiang, G. A. Ameer and M. R. Kibbe, *J. Controlled Release*, 2018, **274**, 69–80.
28 R. van Lith, E. K. Gregory, J. Yang, M. R. Kibbe and G. A. Ameer, *Biomaterials*, 2014, **35**, 8113–8122.
29 R. van Lith, X. S. Wang and G. Ameer, *ACS Biomater. Sci. Eng.*, 2016, **2**, 268–277.
30 L. Yu, W. He, E. B. Peters, B. T. Ledford, D. N. Tsihlis and M. R. Kibbe, *ACS Appl. Bio Mater.*, 2020, **3**, 2150–2159.
31 R. Aguirre and J. M. May, *Pharmacol. Ther.*, 2008, **119**, 96–103.
32 J. M. May and F. E. Harrison, *Antioxid. Redox Signal.*, 2013, **19**, 2068–2083.
33 L. Rossig, J. Hoffmann, B. Hugel, Z. Mallat, A. Haase, J. M. Freyssinet, A. Tedgui, A. Aicher, A. M. Zeiher and S. Dimmeler, *Circulation*, 2001, **104**, 2182–2187.
34 G. Ulrich-Merzenich, C. Metzner, B. Schiermeyer and H. Vetter, *Eur. J. Nutr.*, 2002, **41**, 27–34.
35 S. Kawashima and M. Yokoyama, *Arterioscler. Thromb. Vasc. Biol.*, 2004, **24**, 998–1005.
36 B. Hornig, N. Arakawa, C. Kohler and H. Drexler, *Circulation*, 1998, **97**, 363–368.
37 S. Taddei, A. Virdis, L. Ghiadoni, A. Magagna and A. Salvetti, *Circulation*, 1998, **97**, 2222–2229.
38 S. Gluhih, A. Kovalov, A. Tishkunov, P. Akishin, A. Chate, E. Auzins and M. Kalnins, *Mech. Compos. Mater.*, 2012, **48**, 57–64.
39 E. K. Gregory, J. M. Vercammen, M. E. Flynn and M. R. Kibbe, *J. Vasc. Surg.*, 2016, **64**, 1835–1846.
40 C. A. Serrano, Y. Zhang, J. Yang and K. A. Schug, *Rapid Commun. Mass Spectrom.*, 2011, **25**, 1152–1158.
41 J. Yang, A. R. Webb and G. A. Ameer, *Adv. Mater.*, 2004, **16**, 511–516.
42 M. C. Serrano, E. J. Chung and G. A. Ameer, *Adv. Funct. Mater.*, 2010, **20**, 192–208.
43 A. P. Ebrahimi, *J. Vasc. Interv. Neurol.*, 2009, **2**, 155–162.
44 A. B. Shephard, S. C. Nichols and A. Braithwaite, *Talanta*, 1999, **48**, 607–622.
45 L. C. Xu, J. W. Bauer and C. A. Siedlecki, *Colloids Surf., B*, 2014, **124**, 49–68.
46 I. Jialal and S. M. Grundy, *J. Clin. Invest.*, 1991, **87**, 597–601.
47 E. B. Kurutas, *Nutr. J.*, 2016, **15**, 22.
48 A. de Mel, F. Murad and A. M. Seifalian, *Chem. Rev.*, 2011, **111**, 5742–5767.
49 A. J. Holmes and D. L. H. Williams, *J. Chem. Soc., Perkin Trans. 2*, 2000, 1639–1644.
50 T. P. Dasgupta and J. N. Smith, in *Nitric Oxide, Pt D: Nitric Oxide Detection, Mitochondria and Cell Functions, and Peroxynitrite Reactions*, ed. E. Cadenas and L. Packer, Elsevier Academic Press Inc, San Diego, 2002, vol. 359, pp. 219–229.
51 A. Kytzia, H. G. Korth, R. Sustmann, H. de Groot and M. Kirsch, *Chem. – Eur. J.*, 2006, **12**, 8786–8797.
52 S. A. Suarez, N. I. Neuman, M. Munoz, L. Alvarez, D. E. Bikiel, C. D. Brondino, I. Ivanovic–Burmazovic, J. L. Miljkovic, M. R. Filipovic, M. A. Marti and F. Doctorovich, *J. Am. Chem. Soc.*, 2015, **137**, 4720–4727.
53 N. D. Tsihlis, J. Murar, M. R. Kapadia, S. S. Ahanchi, C. S. Oustwani, J. E. Saavedra, L. K. Keefer and M. R. Kibbe, *J. Vasc. Surg.*, 2010, **51**, 1248–1259.
54 C. E. Cooper, *Biochim. Biophys. Acta, Bioenerg.*, 1999, **1411**, 290–309.
55 J. Du, J. J. Cullen and G. R. Buettner, *Biochim. Biophys. Acta, Rev. Cancer*, 2012, **1826**, 443–457.
56 B. C. Yi, Y. B. Shen, H. Tang, X. L. Wang and Y. Z. Zhang, *Acta Biomater.*, 2020, **108**, 237–249.
57 J. H. Pang, Y. Farhatnia, F. Godarzi, A. Tan, J. Rajadas, B. G. Cousins and A. M. Seifalian, *Small*, 2015, **11**, 6248–6264.
58 Y. H. Ma, S. H. Ling and H. E. Ives, *Biochem. Biophys. Res. Commun.*, 1999, **265**, 606–610.
59 C. H. Li, Y. H. Hu, M. Mayr and Q. B. Xu, *J. Biol. Chem.*, 1999, **274**, 25273–25280.
60 N. L'Heureux, S. Paquet, R. Labbe, L. Germain and F. A. Auger, *FASEB J.*, 1998, **12**, 47–56.
61 M. A. Contreras, W. C. Quist and F. W. LoGerfo, *Microsurgery*, 2000, **20**, 15–21.
62 Z. Zhang, Z. X. Wang, S. Q. Liu and M. Kodama, *Biomaterials*, 2004, **25**, 177–187.
63 G. Drouin, J. R. Godin and B. Page, *Curr. Genomics*, 2011, **12**, 371–378.
64 R. C. Morales, E. S. M. Bahnson, G. E. Havelka, N. Cantu-Medellin, E. E. Kelley and M. R. Kibbe, *Redox Biol.*, 2015, **4**, 226–233.
65 D. F. Wang, Y. Y. Xu, L. Q. Li and L. S. Turng, *J. Mater. Chem. B*, 2020, **8**, 1801–1822.
66 Y. Jeong, Y. Yao and E. K. F. Yim, *Biomater. Sci.*, 2020, **8**, 4383–4395.